ORIGINAL ARTICLE
Iran J Allergy Asthma Immunol
August 2025; 24(4):481-497.
DOI:10.18502/ijaai.v24i4.19129

MicroRNA-148a-3p Regulates Colorectal Cancer Cell Proliferation and Immune Escape through KLF4

Chunlei Zhang[1], Shiming Yi[2], Xiansheng Cao[3], and Jiafeng Wang[4]

[1] Department of Colorectal and Anus Surgery, Yantai Affiliated Hospital of Binzhou Medical University, Yantai, China
[2] Department of Hepatobiliary Surgery, Yantai Affiliated Hospital of Binzhou Medical University, Yantai, China
[3] Department of Gastrointestinal Surgery, Hernia and Abdominal Wall Surgery Ⅰ, Yantai Affiliated Hospital of Binzhou Medical University, Yantai, China
[4] Department of General Surgery, Tai'an City Central Hospital, Tai'an, China

Received: 22 October 2024; Received in revised form: 10 December 2024; Accepted: 25 December 2024

ABSTRACT

MicroRNA (miR)-148a-3p is most frequently upregulated in solid tumors, such as colorectal cancer (CRC). This study aimed to elucidate the role of miR-148a-3p in CRC cell proliferation and immune escape and its potential mechanism.

miR-148a-3p and Kruppel-like transcription factor 4 (*KLF4*) expressions were quantified by western blot and quantitative real-time polymerase chain reaction (qRT-PCR). The proliferation, migration, invasion, epithelial-mesenchymal transition (EMT), and immune evasion abilities of CRC cells were evaluated with the cell counting kit-8 assay, Transwell, western blot, and enzyme-linked immunosorbent assays. The proliferation or apoptosis of $CD8^+$ and $CD4^+$ T cells after coculture with CRC cells was assessed by flow cytometry. Dual-luciferase reporter gene testing was used to validate the targeting association between *KLF4* and miR-148a-3p. A nude mouse subcutaneous graft tumor model was constructed, and $CD8^+$ T cell infiltration was detected by immunohistochemistry and flow cytometry.

miR-148a-3p exhibited a high level, while *KLF4* was under-expressed in CRC cells; miR-148a-3p negatively regulated the *KLF4* level. Overexpression of miR-148a-3p enhanced CRC cell proliferation, migration, invasion, EMT, and immune escape; silencing miR-148a-3p caused the opposite trend; moreover, the said biological functions of CRC cells were weakened with overexpression of *KLF4* but enhanced with silencing of *KLF4*; silencing *KLF4* weakened the influences of dampened miR-148a-3p on CRC development. Silencing miR-148a-3p promoted the infiltration of $CD8^+$ T cells and inhibited tumor growth.

In summary, miR-148a-3p promotes CRC cell proliferation and immune evasion by regulating the expression of *KLF4*. This finding can be used for reference when developing a new way of CRC treatment.

Keywords: Cell proliferation; Colorectal cancer; Immune escape; Kruppel-like transcription factor 4; MicroRNA-148a-3p

Corresponding Author: Jiafeng Wang, PhD;
Department of General Surgery, Tai'an City Central Hospital, Tai'an, China. Tel: (+98 133) 7538 1630, Email: doctorwangjf@126.com

INTRODUCTION

Colorectal cancer (CRC) stands as one of the most prevalent cancer types leading to mortality in humans.[1,2] All over the world in 2020, the number of people who died from CRC ranked second among those who died from cancers.[3] Due to the rise in population who have bad habits in lifestyle and diet, an increasing number of Chinese people are affected by CRC.[4] When being diagnosed, more than 83% of CRC patients have entered the later period, with almost half of these patients experiencing metastasis to other parts of the body, resulting in a poor prediction of the disease.[5] Once CRC cells migrate, propagate, attack, or reappear, the proportion of these patients who survive within 5 years will not exceed 30%.[6,7] To control CRC, it is pressing to identify therapeutic targets having a causal relationship with this disease, as well as biomarkers easily measurable and pertaining to clinical outcomes. As already proved,[8,9] microRNAs (miR) meet these requirements. As a critical factor determining the regulation posttranscription, microRNAs not only participate in the evolution of a cancer but also modulate the anticancer immune response.[10-12] Regulating the microRNA expression has become a novel strategy for cancer therapy.

Located on chromosome 7p15.2, miR-148a-3p probably possesses a stem-loop structured sequence;[13] it results from the cleavage at the 3′ end of pre-microRNA by Dicer.[14] As discovered in a previous study, miR-148a-3p levels are upregulated in both endometrial cancer[15] and CRC.[16] Other studies[17-22] have also demonstrated that miR-148a-3p is a microRNA suppressive for tumors, with its expression dampened in breast cancer, gastric cancer, epithelial ovarian cancer, hepatocellular carcinoma, and pancreatic cancer. This reveals that miR-148a-3p holds tissue specificity and plays varying roles in different tumors, offering more possibilities to study miR-148a-3p. As found in this survey, Kruppel-like factor 4 (KLF4) is gene-targeted and affected by miR-148a-3p; KLF4 may be an effective target for miR-148a-3p-based regulation in CRC cells.

Being a transcription factor specific to epithelial cells, KLF4 can modulate the expression of cytokines, taking a crucial part in inflammatory responses;[23-25] it can also stimulate immune cells (e.g., $CD8^+$ T) to perform antitumor immune regulation,[26] thereby interfering with the development of malignant tumors. Numerous articles have described that KLF4 is a potential CRC-suppressive gene regulated by microRNAs and is capable of inhibiting CRC cells from propagating and migrating.[27-32] Yet, no article has mentioned the immune regulatory role of KLF4 in CRC cells.

As demonstrated in this research, KLF4 exhibited a CRC-suppressive effect and was under the control of miR-148a-3p; miR-148a-3p, once expressed at an excess level, facilitated CRC cells to propagate and evade immunization. These findings prove that miR-148a-3p targets KLF4 to regulate CRC cells' biological functions, making miR-148a-3p/KLF4 an available marker and target spot for treating CRC.

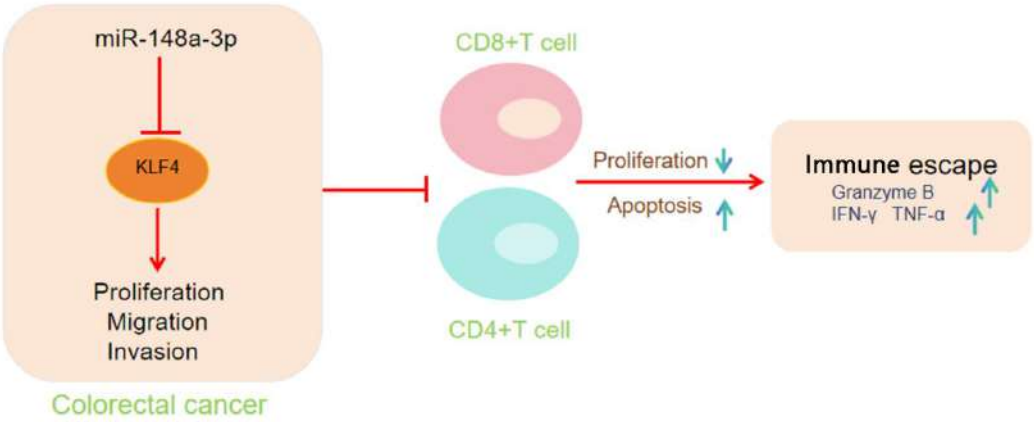

Graphical abstract. MicroRNA-148a-3p promoted colorectal cancer (CRC) cell proliferation, invasion, and metastasis by negatively targeting and regulating KLF4. In addition, overexpression of miR-148a-3p reduced the antitumor effect of effector T cells ($CD8^+$ and $CD4^+$), suppressed their proliferation, and promoted their apoptosis, which in turn promoted the immune escape of CRC cells.

MATERIALS AND METHODS

Cell Culture

Normal colon epithelial cells NCM460 and CRC cell lines (SW620, LoVo, and HT29) of human used in this research were all collected from the Cell Bank of Chinese Academy of Sciences (Shanghai, China). After that, the cells were soaked in a RPIM-1640 medium (ORCPM0110B, ORiCells Biotechnology, Shanghai, China) and cultured in a setting of 37℃ and 5% CO_2. The medium was previously blended with 10% fetal bovine serum (C0235, Beyotime, Shanghai, China), 100 μg/mL streptomycin, and 100 U/mL penicillin (ST488S, Beyotime, Shanghai, China).

Cell Transfection and Treatment

The cells were subcultured when reaching a monolayer confluency and collected for transfection testing when entering the log phase. For transfection, miR-148a-3p mimics/inhibitors (mimics/inhibitors) and their negative controls (mimic-NC/inhibitor-NC), as well as over-expressed/silenced KLF4 (OE-KLF4/Si-KLF4) and its negative control OE-NC/Si-NC, were acquired from Ribobio (Guangzhou, China). Then, Lipofectamine 3000 (L3000001, Invitrogen, Austin, TX, USA) was applied, following its user manual, to have the said testing vectors and control vectors transfected into CRC cells, respectively. Afterward, the cells were subjected to 48-hour incubation in an incubator before doing the subsequent tests.

CRC cells transfected with mimics-NC or mimics were recorded as the mimic-NC or mimics group. CRC cells transfected with inhibitor-NC or inhibitor were recorded as inhibitor-NC or inhibitor group. CRC cells transfected with OE-NC or OE-KLF4 were designated as OE-NC or OE-KLF4 groups. CRC cells transfected with Si-NC or Si-KLF4 were designated as Si-NC or Si-KLF4 groups. In addition, CRC cells co-transfected with the inhibitor and Si-KLF4 were designated as the inhibitor Si-KLF4 group.

Isolation of Peripheral Blood $CD8^+$ T Cells and $CD4^+$ T Cells

Fasting healthy blood donors were collected 10 mL of venous blood, diluted in an equal volume of PBS, and added to human peripheral blood lymphocyte isolation solution (C0025, Beyotime, Shanghai, China). Following low-speed centrifugation, the white film at the liquid interface is the peripheral blood mononuclear cells (PBMCs). After centrifugation at a low speed, the white membrane at the interface of the plasma and the layered solution was aspirated, which is the peripheral blood mononuclear cells. Cells were sorted through the $CD8^+$ T cell sorting kit (11348D, Invitrogen, Austin, TX, USA) and the $CD4^+$ T cell sorting kit (11346D, Invitrogen, Austin, TX, USA). PBMCs (about 1×10^7) were taken, centrifuged, and the cells were resuspended in PBS buffer. A biotin-labeled antibody (10 μL) was added, mixed well, and reacted at 4°C for 5 minutes. Added 30 μL PBS and 20 μL $CD8^+$ T cell or $CD4^+$ T cell microsphere antibody, mixed well, and reacted for 10 min. The unlabeled cells that passed through the separation column were collected as enriched $CD8^+$ T cells or $CD4^+$ T cells.

Using Transwell (Corning Incorporated, Corning, NY, USA) and 24-well plates, $CD8^+$ T and $CD4^+$ T cells were co-cultured with CRC cells having a low/high miR-148a-3p level or a low/high KLF4 level at a 15:1 ratio (effector T cells: tumor target cells) for 45 hours (effector T cells in the upper chamber, CRC cells in the lower chamber) at 37℃.[33] Following coculturing, the CRC cells, effector T cells, and coculture supernatant were gathered for later use.

Cell Counting Kit-8 (CCK-8) Tests

Cell activity: The activity of cells was tested following the instructions attached with the applicable assay kit (C0038, Beyotime, Shanghai, China). Cells (5×10^3 cells/mL) were injected into a 96-well plate. Respectively 1, 2, 3, and 4 days later, each well was dosed with 10 μL of CCK-8 reagent for 4-hour cell cultivation at 37℃. Thereafter, a microplate reader was employed to test the optical density (OD) of cells at a wavelength of 450 nm.

Additionally, collected tumor cells after co-culture with effector T cells, applied CCK-8 assay kit to evaluate the destructive impact of effector T cells on the tumor target cells; the final percentage of dead cells (Tumor Lysis, %) was calculated based on the absorbance readings.[34]

Carboxyfluorescein Diacetate Succinimidyl Ester (CFSE) Staining

1 μL of CFSE probe (C1031, Beyotime, Shanghai, China) was added to each milliliter of $CD8^+$ T/$CD4^+$ T cells suspension (density of 1.0×10^6/mL) to give a final

Published by Tehran University of Medical Sciences (http://ijaai.tums.ac.ir)

concentration of 5 μM, and subsequently incubated at 37°C for 10 minutes to facilitate labeling. Terminated the staining by adding 5 times the volume of medium and mixing well. The cells were centrifuged, washed 2 times with PBS to remove unbound CFSE solution. Resuspend with PBS buffer, take a small number of drops, and add them to the 96-well plate, and observe under the fluorescence microscope to see if the labeling is successful. CFSE pre-stained $CD8^+$ T cells/$CD4^+$ T cells were taken and co-cultured with CRC cells for 48 h. Cell proliferation of $CD8^+$ T cells/$CD4^+$ T cells was detected through a flow cytometer (BD FACSCaliburTM, BD Biosciences, San Jose, CA, USA).

Flow Cytometry

$CD8^+$ T cells/$CD4^+$ T cells were co-incubated with CRC cells using Transwell for 48 h, collected, rinsed twice with PBS, and gently mixed by adding 500 μL Binding Buffer. Then propidium iodide and Annexin-V-FITC (C1062S, Beyotime, Shanghai, China) were introduced and left to incubate for 15 min away from light. $CD8^+$ T cells/$CD4^+$ T cells apoptosis was tested using a flow cytometer, and the experimental results were analyzed and counted by FlowJo software (v10.8, BD Biosciences, San Jose, CA, USA).

ELISA

This testing was to make clear the contents of cytokines in the supernatants after co-culture. ELISA kits for tumor necrosis factor (TNF-α, ab181421), Interferon-γ (IFN-γ, ab224197), and Granzyme B (ab235635) were all purchased from Abcam (Waltham, MA, USA). Following the instructions, we diluted the co-culture supernatants and added 100 μL of the suspension to the assay plate, waiting for a 1.5-hour incubation at 37°C. Next, the plate was dosed with 100 μL of relevant antibodies, incubating for 1.5 hours at 37°C for cell incubation. Next, the plate was injected with 100 μL of Streptavidin-Horseradish Peroxidase conjugate (Streptavidin-HRP, S911, Invitrogen, Austin, TX, USA) for half an hour of cell incubation at 37°C. Subsequently, 100 μL of color reagent solution was dosed to the plate, followed by 15-minute incubation in a setting without light. Thereafter, 100 μL of stop buffer was added to the plate to block the reaction. Finally, we used a microplate reader to assess the OD_{450} of the samples and calculate their concentrations.

Transwell Testing

Cell movement capacity testing: Transwell chambers were placed above a 24-well plate. Cell suspension (100 μL, 1×10^5 cells/mL) was introduced into each chamber; each well below the chamber was filled with RPMI-1640 medium (500 μL, with 10% FBS); the plate was then put into an incubator (setting: 37°C; 5% CO_2) for 24 hours of cell culture. After that, the culture medium in both chambers was abandoned; cotton swabs were used to gently remove the cells in the upper section. Subsequently, cells in the lower chamber were administered with a solution containing 4% paraformaldehyde (P6148, Sigma, St. Louis, MO, USA) for 30-minute fixation. Subsequently, the cells were colored with 0.1% crystal violet (C0121, Beyotime, Shanghai, China) for 30 minutes. Following two washes using PBS and drying up, a high-power microscope was utilized to observe and capture images of the cells. Finally, the movement capacity of the cells was determined as on the number of moved cells observed under the microscope.

Cell attacking capacity testing: First, 50 μL of Matrigel (354234, Corning Inc., Corning, NY, USA) was placed in the Transwell chamber in advance and air dried for 4 hours at the indoor temperature. Next, cell suspension and culture medium were injected into the Transwell chambers and the wells of a 24-well plate below the chambers, respectively, following the same operation steps as the cell movement capacity testing.

Bioinformatics Analysis

According to the microRNA target prediction database TargetScan (http://www.targetscan.org/), KLF4 was predicted as the target gene of miR-148a-3p. Based on this prediction, the correlation between miR-148a-3p and KLF4 was verified by Pearson analysis.

Dual-luciferase Reporter Gene Testing

Based on the above prediction findings, such as wild-type fragment KLF4-WT and mutant-type fragment KLF4-MUT in the 3'UTR region of KLF4, binding with the miR-148a-3p sequence was cloned and inserted into dual-luciferase reporter gene vectors (E1330, Promega, Madison, WI, USA). Then, Lipofectamine 3000 was utilized to have KLF4-WT and KLF4-MUT recombinant plasmid vectors, together with miR-148a-3p mimic and mimic-NC, transfected into CRC cells. After 48-hour transfection, the cells were collected separately and tested with an applicable kit (RG027,

Beyotime, Shanghai, China) following its instructions to acquire the activity of the luciferase reporter gene.

Subcutaneous Tumor Model

Healthy BALB/c nude mice were obtained from Vitalriver (Beijing, China) and acclimatized for one week at a constant temperature of 22℃. Each group consisted of six mice, selected randomly to form the six groups. Each nude mouse received a subcutaneous injection of 200 μL of LoVo cell suspension (5×10^5 cells/mouse) transfected with inhibitor-NC, inhibitor, Si-NC, Si-KLF4, inhibitor-NC+Si-NC, or inhibitor+Si-KLF4 in the right axilla, respectively. The size of the subcutaneous tumor was assessed using vernier calipers every week to calculate the tumor volume. On day 28, the mice were anesthetized and executed, and the tumors were completely peeled off by tissue clippers, weighed, and photographed to record the mass of the tumors.

qRT-PCR

To extract total RNA, cells and tumor tissues were treated with TRIzol reagent kit (DP424, TIANGEN, Beijing, China). Then, cDNA synthesis was completed by adding Prime Script RT reagent kit (RR047A, Takara, Tokyo, Japan) to the extracted total RNA. Followed by, the obtained mixture was added with chloroform at the indoor temperature, followed by the addition of isopropanol and centrifugation, obtaining the precipitated RNA. After that, SYBR Green PCR kit (4309155, Applied Biosystems, DE, USA) was added to the final mixture to make qRT-PCR analysis of miR-148a-3p and KLF4, along with their endogenous controls (U6 and GAPDH), using the ABI PRISM 7300 RT-PCR system (7300, ABI, Carlsbad, CA, USA). At last, the transcription levels were quantified using the $2^{-\Delta\Delta Ct}$ method. The primers adopted the following designs:

miR-148a-3p:
F: 5'-GCGCGTCAGTGCACTACAGAA-3';
R: 5'-AGTGCAGGGTCCGAGGTATT-3';
U6:
F: 5'-CTCGCTTCGGCAGCACAU6-3';
R: 5'-AACGCTTCACGAATTTGCGT-3';
KLF4:
F: 5'-TACCCTCGTTCAGTGGCTCT-3';
R: 5'-CTGACTCTCCTGTCTCCGCTC-3';
GAPDH:
F: 5'-CTAGGCAGCAGCAAGCATTC-3';
R: 5'-AAGGCATGGCTGCAACTGAA-3'.

Western Blot

Cells and tumor tissues were collected and treated for 30 minutes with lysis buffer (20101ES60, Yeasen Biotechnology, Shanghai, China) in a setting of 4℃ to extract proteins. Then, the protein concentrations were tested using the BCA kit (P0012, Beyotime, Shanghai, China). Further, the proteins (50 μg) were separated by treatment with 10% SDS-PAGE and then transferred onto a PVDF membrane. After translocation, the membrane was blocked for 1 hour. Followed by a solution of rabbit-derived primary antibody against KLF4 (1:1000; ab215036; Abcam, Waltham, MA, USA) or against GAPDH (1:2500; ab9485; Abcam, Waltham, MA, USA) was incubated onto the membrane overnight in a setting of 4℃. Following washes with TBST, the membrane was further incubated for another 30 minutes with a solution of goat anti-rabbit IgG (1:2000, ab6721, Abcam, Waltham, MA, USA) at the indoor temperature. Afterward, ECL chemiluminescence solution (P0018S, Beyotime, Shanghai, China) was dosed onto the membrane to visualize and expose the protein strips. Subsequently, we took pictures of the protein strips using a chemiluminescence imaging system (5200, Tanon, Shanghai, China) and analyzed the gray values of the protein strips through Image J 1.8.0 software (National Institutes of Health, Bethesda, MD, USA).

Immunohistochemistry

After fixation with 4% paraformaldehyde, tumor tissues were routinely dehydrated, sectioned after paraffin embedding (thickness of 4~5 μm), deparaffinized with xylene (247642, Sigma-Aldrich, St. Louis, MO, USA), and repaired antigen. Sections were treated with a 3% H_2O_2 solution for 25 min. Subsequently, the tissues were evenly covered with drops of 5% bovine serum albumin (ST023, Beyotime, Shanghai, China) and closed for 30 min. CD8 antibody (MA5-14548, 1:100, Invitrogen, Austin, TX, USA) was administered onto the sections and left to incubate at 37°C for 90 minutes. Then, the samples were covered with HRP-labeled secondary antibody (1:10000) for 20 min. DAB (P0203, Beyotime, Shanghai, China) color development, tap water terminated color development. Mayer Hematoxylin (MHS16, Sigma-Aldrich, St. Louis, MO, USA) was re-stained and observed under the microscope.

Published by Tehran University of Medical Sciences (http://ijaai.tums.ac.ir)

Effector T cell marker assay

Mouse tumor tissue was taken and ground thoroughly to prepare a tumor single cell suspension (1.0×10^7/mL). PE-labeled TNF-α antibody (12-7349-41, Invitrogen, Austin, TX, USA), APC-labeled IFN-γ antibody (17-7311-82, Invitrogen, Austin, TX, USA) and Granzyme B antibody (GRB05, Invitrogen, Austin, TX, USA) were added and FITC-labeled CD8 antibody (11-0081-82, Invitrogen, Austin, TX, USA), mixed well and incubated for 30 min away from light. Transferred to a flow cytometer, the percentage of $CD8^+$ T cells was analyzed and counted by FlowJo software.

Data Analysis

All the data are reported as mean value±the standard deviation. Data analysis was conducted with SPSS 26.0 software (SPSS Inc., Chicago, IL, USA). The t-test was employed for two-group comparisons, while one-way ANOVA was used for analyzing differences among multiple groups. $p<0.05$ denotes that there was a large difference.

RESULT

miR-148a-3p Expression in CRC

At the beginning, we searched for miR-148a expression from the TCGA COAD dataset to explore the involvement of miR-148a in human CRC. As depicted in Figure 1A, normal tissues had much lower miR-148a levels than CRC tissues. Besides, miR-148a-3p levels were also tested on normal colon epithelial cells (NCM-460) and CRC cells (SW620, LoVo, and HT29) of humans. The testing results reveal that the *miR-148a-3p* level in CRC cells (particularly in cells LoVo and HT29) was much higher than in cells NCM-460 (Figure 1B). As previously reported, miR-148a-3p may drive the evolution of CRC.

Excess miR-148a-3p's Contribution to CRC Cells' Biological Functions

Considering the high miR-148a-3p contents of cells LoVo and HT29, these two cells were selected for analyzing the biological properties of CRC cells in vitro. Further, mimics and inhibitors were incorporated into the two cells to ascertain miR-148a-3p's impacts on the migration, propagation, and epithelial-mesenchymal transition (EMT) of CRC cells in vitro.

Initially, after being transfected with mimics, CRC cells were tested with the qRT-PCR method to ensure the stable overexpression of *miR-148a-3p* (Figure 2A). Next, CCK-8 tests were conducted to determine the impacts of miR-148a-3p on CRC cell activity. In consequence (Figure 2B), cells LoVo and HT29 became more active as miR-148a-3p reached an excess level. The results of Transwell testing (Figures 2C-2D) demonstrate that miR-148a-3p overexpression boosted cells LoVo and HT29 cells to attack and migrate. After transfection with mimics, CRC cells experienced a decline in the level of E-cadherin, an epithelial phenotype protein related to the EMT, but a rise in the contents of such mesenchymal phenotype proteins as vimentin and N-cadherin (Figure 2E). To examine the influence of miR-148a-3p levels on effector T cell function, we incubated $CD8^+$ T/$CD4^+$ T cells with miR-148a-3p overexpressed CRC cells. The findings indicated a marked decline in the proliferative capacity of effector T cells (Figures 2F–2H) and a significant rise in apoptotic rate (Figures 2I-2K). In addition, the levels of cytokines TNF-α, IFN-γ, and T-cell activation marker granzyme B were notably reduced in $CD8^+$ T/$CD4^+$ T cells after co-culture with miR-148a-3p overexpressed CRC cells (Figures 2L-2N). These findings revealed that miR-148a-3p overexpression inhibited the activation of $CD8^+$ T/$CD4^+$ T cells and promoted the immune escape of CRC cells.

Impairment of the Biological Functions of CRC Cells by Reducing the miR-148a-3p Content

Subsequently, the miR-148a-3p inhibitor was transfected into CRC cells to lower the miR-148a-3p content. *miR-148a-3p* was knocked down notably in both LoVo and HT29 cells, as Figure 3A displays. Contrary to the result of expressing miR-148a-3p over much, knocking down the miR-148a-3p content of CRC cells resulted in weakened activity (Figure 3B), movement, and attacking (Figures 3C-3D) of cells LoVo and HT29, as well as elevated E-cadherin content but lowered Vimentin and N-cadherin contents in the two cells (Figure 3E). Coculturing of $CD8^+$ T cells and $CD4^+$ T cells with CRC cells knocked down miR-148a-3p caused increased proliferation of effector T cells (Figure 3F–H), markedly declined apoptosis rate (Figure 3I-3K), and notably higher levels of TNF-α, IFN-γ, and granzyme B (Figure 3L-3N). Above all, the expressed level of miR-148a-3p posed a strong influence on CRC cells' biological functions: miR-148a-3p, a cancer-promoting factor, facilitated CRC cells to propagate, attack, and migrate, drove cell EMT, and also suppressed effector T cells' antitumor immune responses.

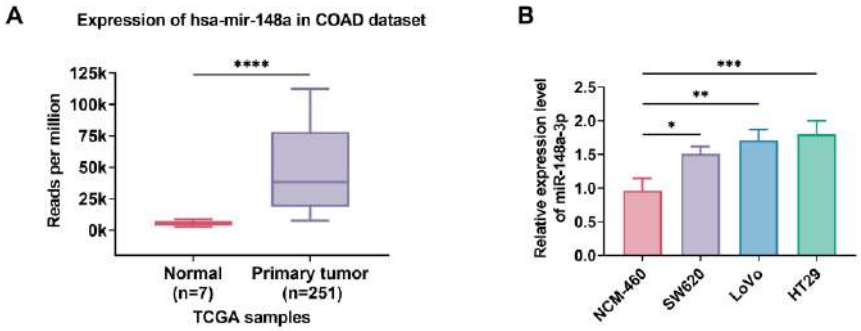

Figure 1. MicroRNA (miR)-148a-3p expression in colorectal cancer (CRC). A. miR-148a level in COAD tissue (n=251) and normal tissue (n=7) samples was analyzed by the TCGA COAD dataset. B. Expressions of miR-148a-3p in varying cell lines. *p<0.05, **p<0.01, ***p<0.001, ****p<0.0001

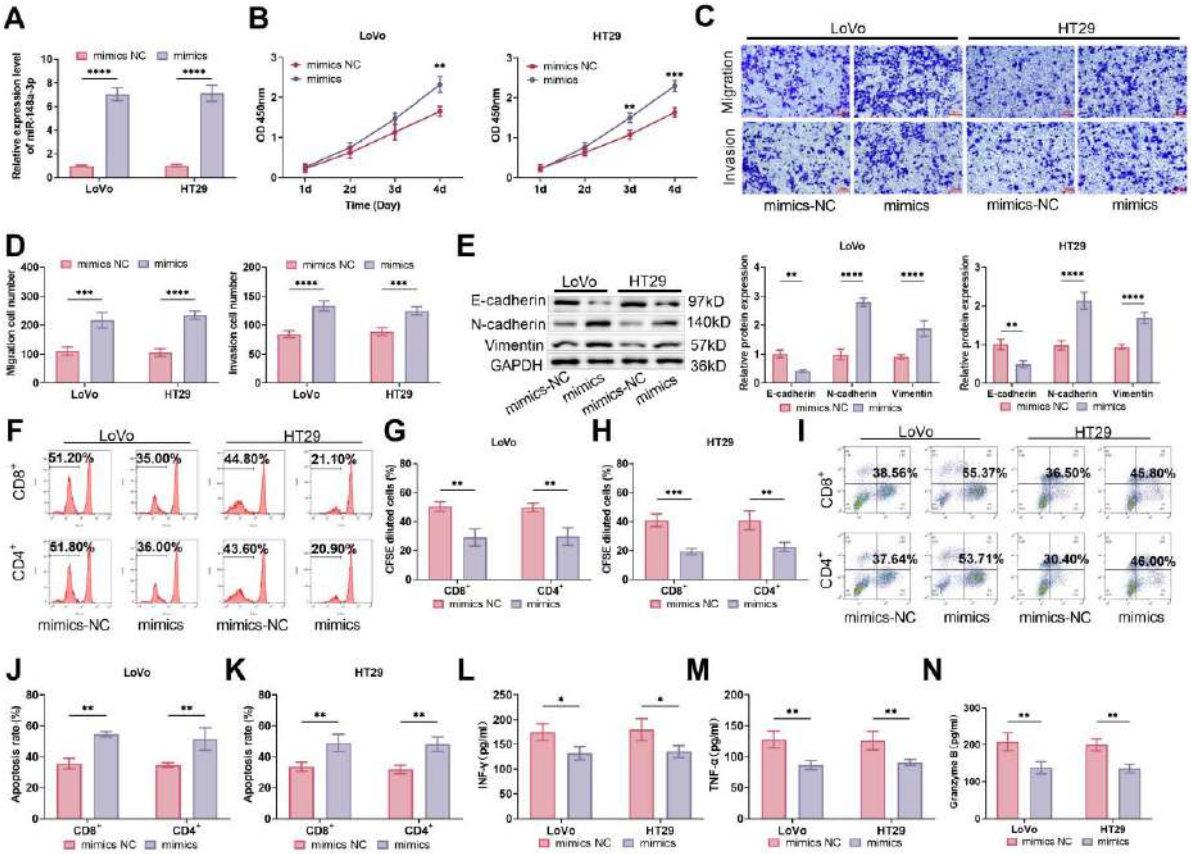

Figure 2. Excess microRNA (miR)-148a-3p's influence on colorectal cancer (CRC) cells' biological behaviors. A. After transfection of mimics NC or mimics, *miR-148a-3p* level in CRC cell lines was detected via qRT-PCR. B. Cell activities were assessed by the cell counting kit-8 (CCK-8) assay. C-D. Cell migration and attacking capacities were tested through Transwell (20×, bar=100 μm). E. Examining epithelial-mesenchymal transition (EMT) marker proteins (Vimentin, N-cadherin, and E-cadherin) levels in CRC cells via western blot. F-H. Proliferative capacity of $CD8^+$ T and $CD4^+$ T cells after co-culture with CRC cells (transfected with mimics NC or mimics) was examined by Carboxyfluorescein Diacetate Succinimidyl Ester (CFSE) staining. I-K. After co-culture with CRC cells, the apoptosis rates of effector T cells were determined by flow cytometry. L-N. The levels of interferon-γ (IFN-γ), tumor necrosis factor-α (TNF-α), and Granzyme B in the co-cultured supernatant were evaluated by enzyme-linked immunosorbent assay. *p<0.05, **p<0.01, ***p<0.001, ****p<0.0001

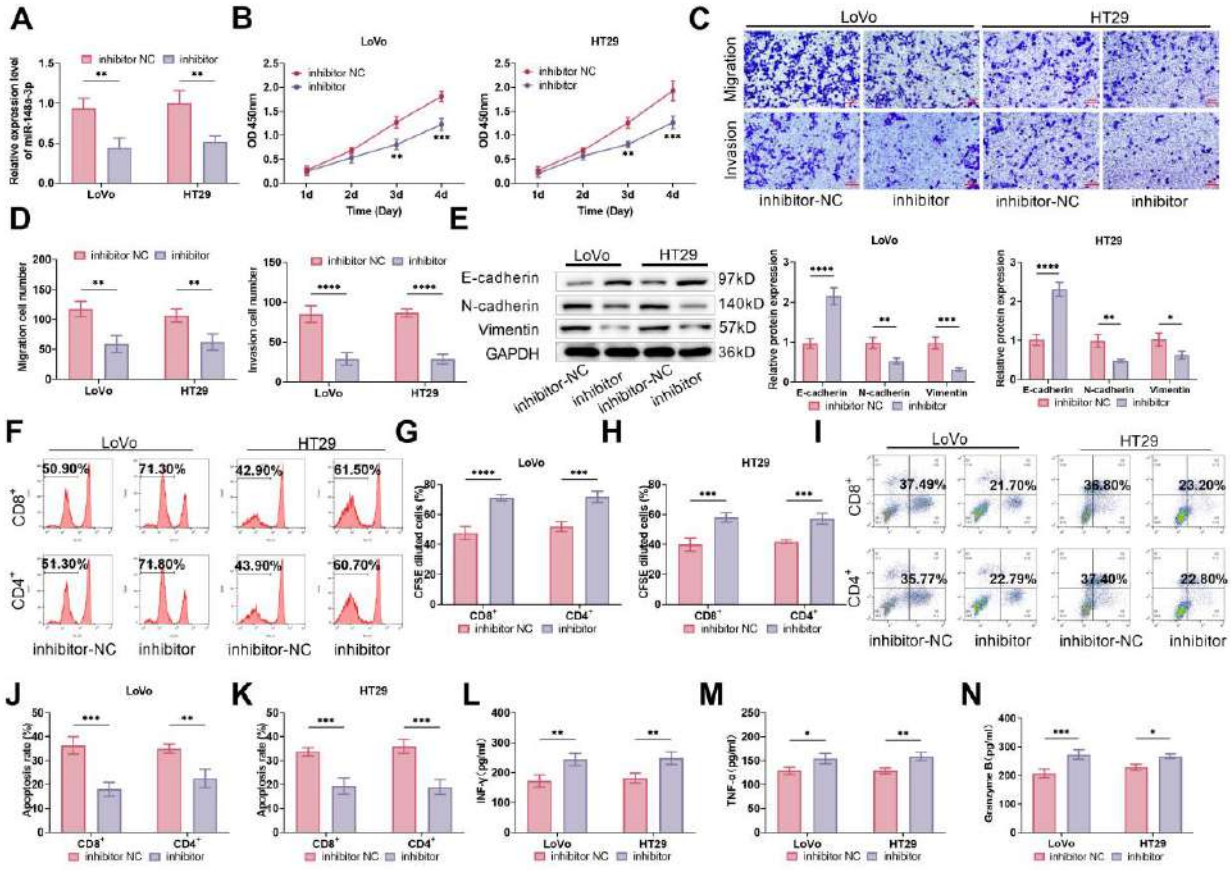

Figure 3. Impairment of colorectal cancer (CRC) cells' biological functions by dampening the microRNA (miR)-148a-3p expression. A. After transfection of inhibitor NC or inhibitor, the expression of *miR-148a-3p* in CRC cell lines was assessed by qRT-PCR. B. Cell activities were assessed by the cell counting kit-8 (CCK-8) assay. C–D. Cell migration and attacking capacities determined by Transwell testing (20×, bar=100 μm). E. The expressions of epithelial-mesenchymal transition (EMT) marker proteins were assessed through western blot testing. F–H. Proliferative capacity of $CD8^+$ T and $CD4^+$ T cells after co-culture with CRC cells (transfected with inhibitor NC or inhibitor) was examined by Carboxyfluorescein Diacetate Succinimidyl Ester (CFSE) staining. I–K. After co-culture with CRC cells, the apoptosis rates of effector T cells were evaluated by flow cytometry. L–N. The levels of interferon-γ (IFN-γ), tumor necrosis factor-α (TNF-α), and Granzyme B in the co-cultured supernatant were evaluated by enzyme-linked immunosorbent assay. *p<0.05, **p<0.01, ***p<0.001, ****p<0.0001

miR-148a-3p's Targeted Suppressive Effect on KLF4

As predicted using the TargetScan database, miR-148a-3p targets the KLF4 gene; the site where miR-148a-3p attaches to KLF4 3'UTR is presented in Figure 4A. To further confirm this prediction, LoVo and HT29 cells were tested with the dual-luciferase reporter gene testing method. Consequently, miR-148a-3p, when expressed at an excess level, suppressed the luciferase activity of the KLF4-WT reporter gene in both of the 2 cell lines, while that of the KLF4-WUT reporter gene showed no significant change (Figure 4B). Besides, miR-148a-3p, when reaching an excess level, dampened the expression of KLF4 in CRC cells, while when reaching a lower level, it heightened the KLF4 expression (Figures 4C–D). The consequences of the Pearson correlation analysis (Figure 4E) imply that miR-148a-3p has a negative correlation with KLF4. These data demonstrated that KLF4 was regulated by miR-148a-3p in a negative and targeted manner and might suppress the advancement of CRC cells.

Attenuation of the Normal Living Activities of CRC Cells by Heightening the KLF4 Expression

To verify whether KLF4 indeed promotes the vital activities of CRC cells in vitro, Over-expressed plasmids OE-KLF4 and silenced plasmids Si-KLF4 were utilized to modulate the content of KLF4 in CRC cells. After transfection with OE-KLF4, we monitored a high rise in the KLF4 level of both cells, LoVo and HT29 (Figures 5A-5B). The elevated KLF4 level further weakened CRC cells' activity (Figure 5C), attacking, migration (Figures 5D-5E), and EMT extent (evidenced by the increased E-cadherin content and declined N-cadherin and Vimentin contents as shown in Figure 5F); the overexpressed KLF4 also promoted the proliferation of $CD8^+$ T/$CD4^+$ T cells (Figures 5G–I), caused a notably lower apoptosis rate these two kinds of cells (Figures 5J–L), and markedly higher levels of TNF-α, IFN-γ, and granzyme B (Figures 5M–O). This phenomenon proved that excess KLF4 indeed retarded CRC cells' normal living activities *in vitro*, and enhanced the immunologic impacts of effector T cells. Followed by an exploration was made into the effect of silenced KLF4 on CRC cells.

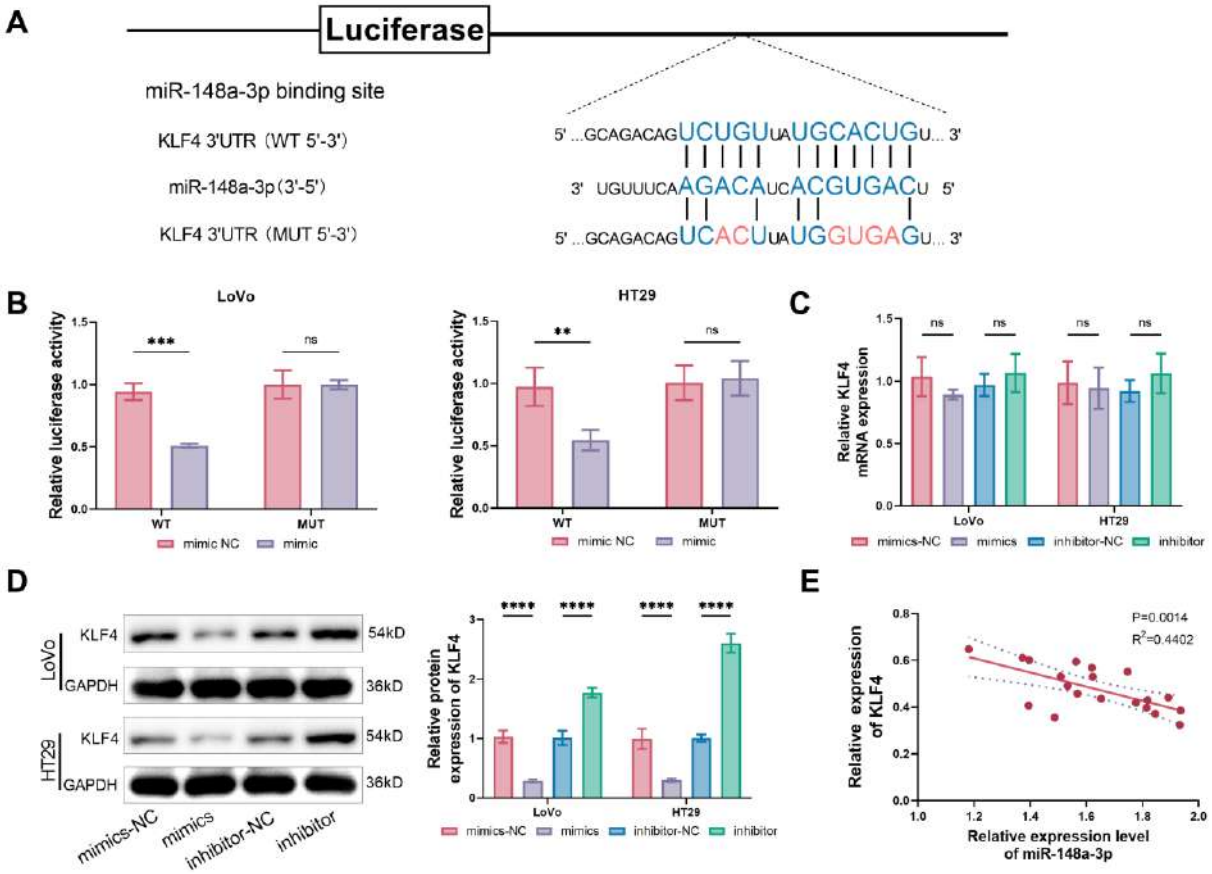

Figure 4. MicroRNA (miR)-148a-3p's targeted regulation of kruppel-like transcription factor 4 (KLF4). A. The attaching site between miR-148a-3p and KLF4 3'UTR. B. Dual-luciferase reporter gene testing results. C. *KLF4* mRNA expression in colorectal cancer (CRC) cells was analyzed by qRT-PCR testing. D. KLF4 protein expressions in CRC cells were evaluated through western blot. E. The correlation between miR-148a-3p and KLF4 was affirmed by Pearson analysis. ns=not significant, **p<0.01, ***p<0.001, ****p<0.0001

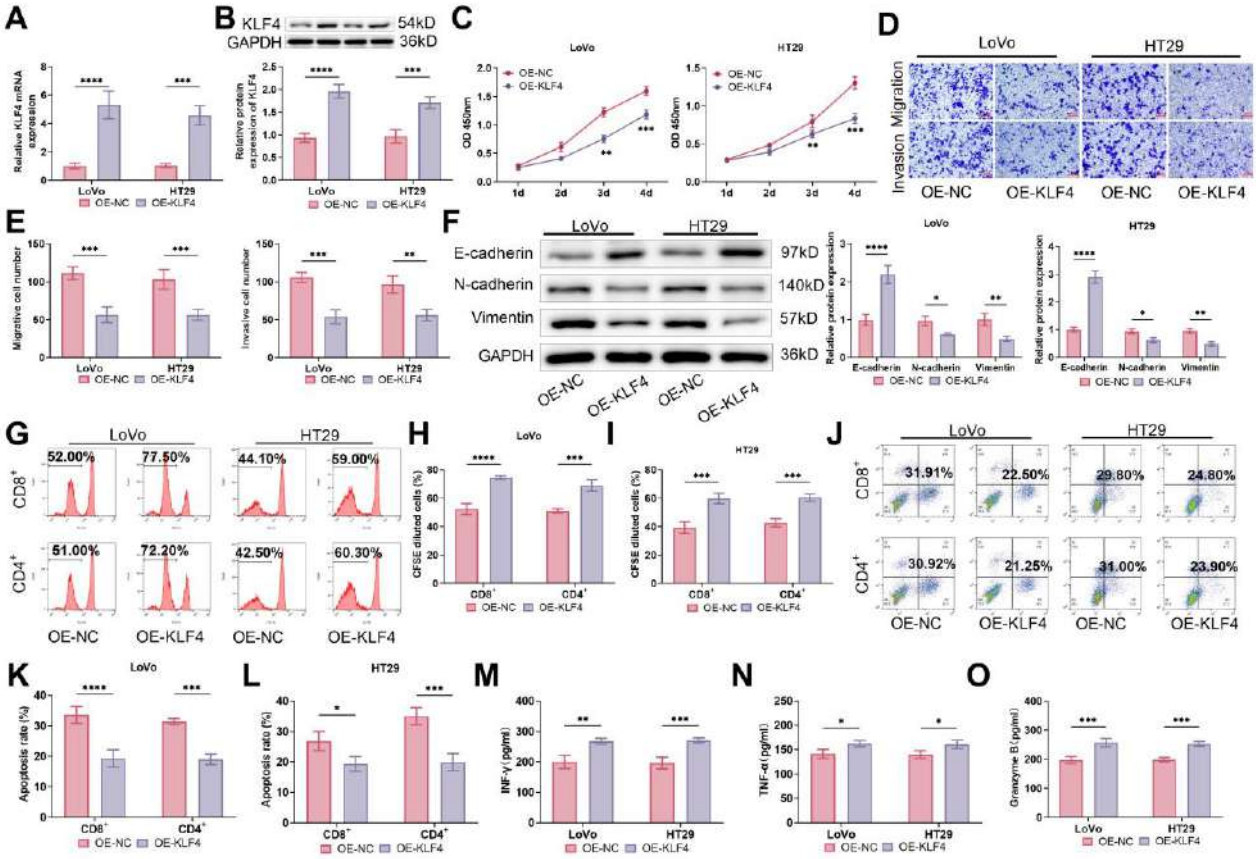

Figure 5. Excess Kruppel-like transcription factor 4 (KLF4)'s impact on the biological behaviors of colorectal cancer (CRC) cells. A–B. After being transfected with OE-KLF4 or OE-NC, to verify the transfection efficiency, qRT-PCR and western blot quantified the level of KLF4. C. Cell activities were determined by the cell counting kit-8 (CCK8) assay. D–E. Cell migration and attacking capacities were evaluated by Transwell testing (20×, bar=100 μm). F. The levels of epithelial-mesenchymal transition (EMT) marker proteins were assessed through western blot testing. G–I. The proliferative capacity of effector T cells after co-culture with CRC cells (transfected with OE-KLF4 or OE-NC) was examined by Carboxyfluorescein Diacetate Succinimidyl Ester (CFSE) staining. J–L. After co-culture with CRC cells, flow cytometry assessed the apoptosis rate of effector T cells. M–O. The contents of interferon-γ (IFN-γ), tumor necrosis factor-α (TNF-α), and granzyme B in the cocultured supernatant were evaluated by enzyme-linked immunosorbent assay. *p<0.05, **p<0.01, ***p<0.001, ****p<0.0001.

Promotion of the Normal Living Activities of CRC Cells by Retarding the KLF4 Expression

Following the same steps as the study of KLF4 overexpression, we first transfected Si-KLF4 into CRC cells and verified the transfection effect through qRT-PCR and western blot testing. In consequence, the KLF4 content in CRC cells was reduced successfully (Figures 6A–B); alongside, cells LoVo and HT29 exhibited enhanced vital force, evidenced by the heightened activity (Figure 6C), migration and attacking capabilities (Figures 6D–E), and EMT extent (Figure 6F) of the two cells, attenuated the proliferative capacity of effector T cells and promoted their apoptosis (Figure 6G–L), which reduced the antitumor immune response (Figure 6M–O). These results demonstrate that KLF4 impeded the normal living activities of CRC cells. In view of this finding, we hypothesized that miR-148a-3p modulated the cell functions in CRC cells by inhibiting KLF4.

KLF4's Partial Counteraction on miR-148a-3p's Effects Against CRC Cells' Development and Immune Suppression

To validate this hypothesis, we designed four groups of experimental LoVo cells: control cells (control group), cells with lowered miR-148a-3p level (inhibitor group), cells with silenced KLF4 (Si-KLF4 group), and cells

with both lowered miR-148a-3p level and silenced KLF4 (inhibitor + Si-KLF4 group) to compare the biological functions of these four cell groups. In comparison, LoVo cells with miR-148a-3p or KLF4 silenced witnessed alleviated or heightened cell activity (Figure 7A), migration, and attacking capacities (Figures 7B–C), as well as boosted or inhibited immune response of $CD8^+$ T cells and $CD4^+$ T cells (Figures 7D-7H). These changes accord with the previous testing results. The biological functions exhibited by the inhibitor+Si-KLF4 group were notably enhanced in comparison to those observed in the inhibitor group, which denotes that Si-KLF4 partially counteracted the dampened miR-148a-3p's effects on CRC cells' evolution and immune suppression; miR-148a-3p in the inhibitor+Si-KLF4 group, in comparison to the Si-KLF4 group, also mitigated the promotional effect of Si-KLF4 on LoVo cells. As KLF4 is known as miR-148a-3p's downstream target gene, the above findings prove that, by targeting KLF4, miR-148a-3p promotes the propagation and immune evasion of CRC cells.

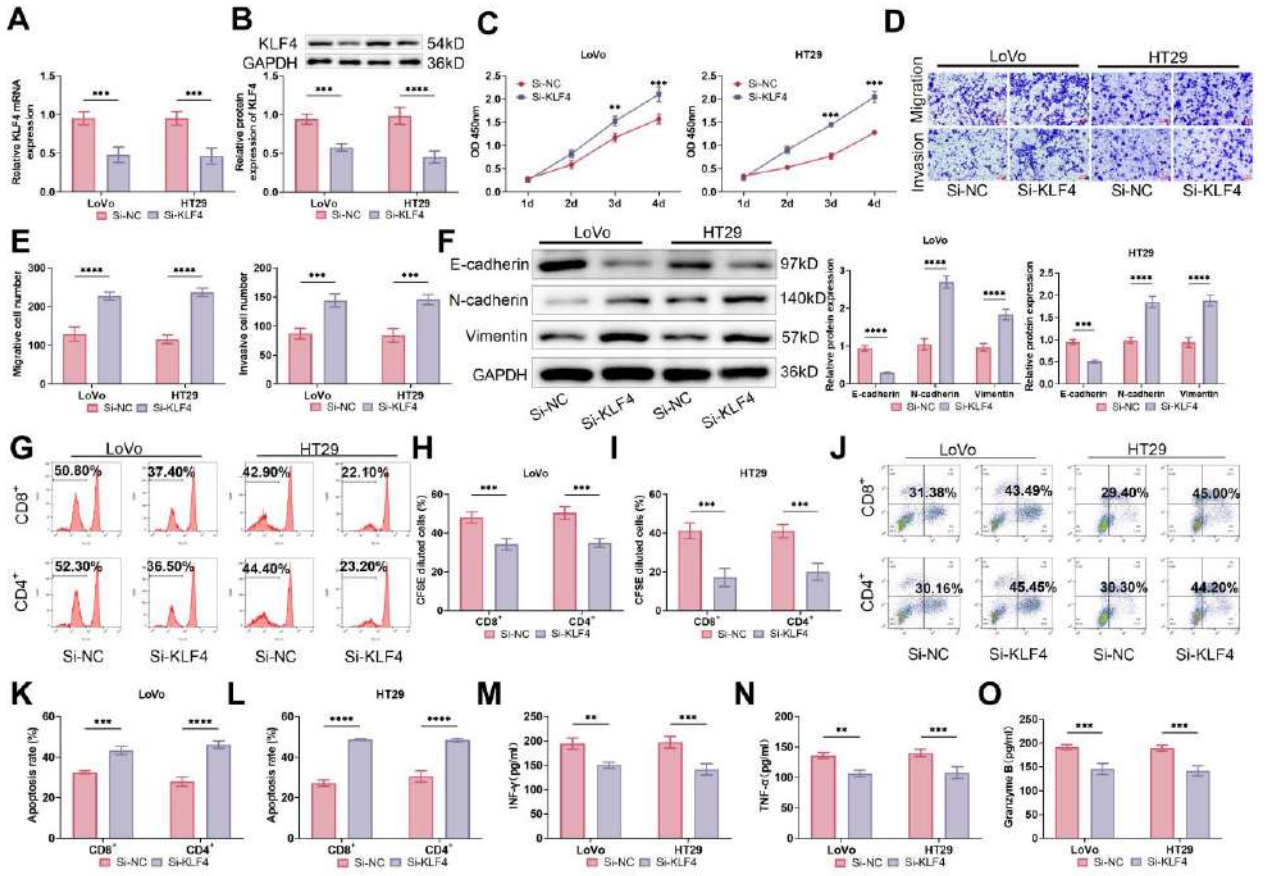

Figure 6. Silenced kruppel-like transcription factor 4 (KLF4) 's impact on the biological behaviors of colorectal cancer (CRC) cells. A–B. After being transfected with Si-NC or Si-KLF4, qRT-PCR and western blot quantified the level of KLF4. C. Cell activities were assessed by cell counting kit-8 (CCK8) assay. D–E Cell migration and attacking capacities were assessed through Transwell testing (20×, bar=100 μm). F. The levels of epithelial-mesenchymal transition (EMT) marker proteins were evaluated by western blot testing. G–I. The proliferative capacity of $CD8^+$ T and $CD4^+$ T cells after co-culture with CRC cells (transfected with Si-NC or Si-KLF4) was examined by Carboxyfluorescein Diacetate Succinimidyl Ester (CFSE) staining. J–L. After coculture with CRC cells, flow cytometry assessed the apoptosis rate of effector T cells. M–O. The contents of interferon-γ (IFN-γ), tumor necrosis factor-α (TNF-α), and granzyme B in the cocultured supernatant were evaluated by enzyme-linked immunosorbent assay. **p<0.01, ***p<0.001, ****p<0.0001.

Published by Tehran University of Medical Sciences (http://ijaai.tums.ac.ir)

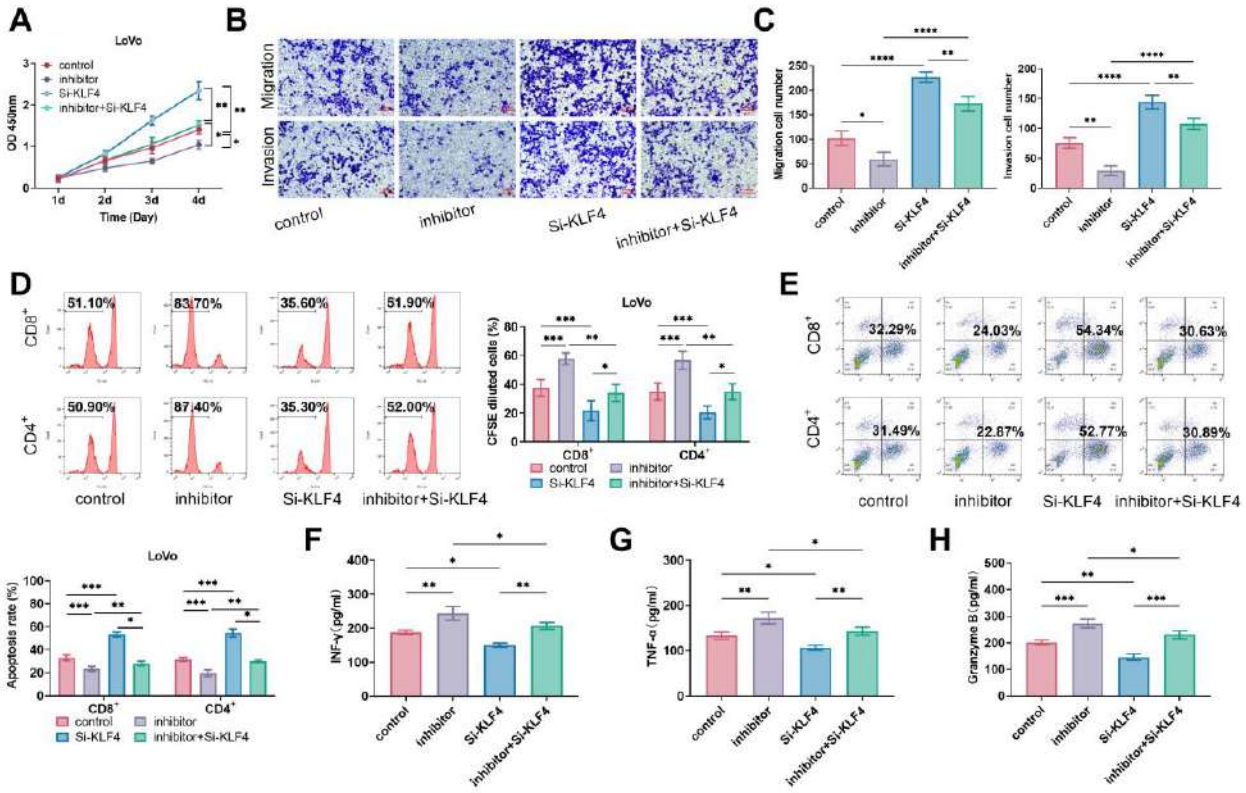

Figure 7. The impacts of microRNA (miR)-148a-3p on colorectal cancer (CRC) cells weakened by kruppel-like transcription factor 4 (KLF4). A. After being transfected with the inhibitor, Si-KLF4 or inhibitor + Si-KLF4, cell activities were assessed by the cell counting kit-8 (CCK8) assay. B–C. Cell migration and attacking capacities assessed with the Transwell testing method (20×, bar=100 μm). D. After coculturing with CRC cells, the proliferative capacity of effector T cells was detected by Carboxyfluorescein Diacetate Succinimidyl Ester (CFSE) staining. E. The apoptosis rate of $CD8^+$ T/ $CD4^+$ T cells was detected by flow cytometry. F–H. The contents of interferon-γ (IFN-γ), tumor necrosis factor-α (TNF-α), and granzyme B in the co-cultured supernatant as evaluated by the enzyme-linked immunosorbent assay. *p<0.05, **p<0.01, ***p<0.001, ****p<0.0001.

Silencing miR-148a-3p inhibits tumorigenicity and immune escape of CRC cells in vivo

Finally, we constructed a subcutaneous transplantation tumor model in nude mice to explore the effects of miR-148a-3p and KLF4 on tumor growth in nude mice in vivo. Injection of LoVo cells transfected with inhibitor or Si-KLF4 significantly reduced the levels of miR-148a-3p and KLF4 in tumors in nude mice in vivo (Figures 8A–B). Silencing miR-148a-3p significantly reduced the volume and weight of tumors in nude mice in vivo compared to the inhibitor-NC + Si-NC (control) group, while silencing KLF4 promoted tumor growth. Tumor volume and weight were significantly higher in the inhibitor+Si-KLF4 group compared to the inhibitor group, suggesting that silencing KLF4 partially impaired the inhibitory effect of silencing miR-148a-3p on tumor growth (Figures 8C–E). Immunohistochemistry and flow cytometry results showed that silencing of miR-148a-3p resulted in increased CD8 positivity and a significantly higher proportion of activated $CD8^+$ T cells in tumor tissues, whereas silencing of KLF4 attenuated the effect of silencing of miR-148a-3p, reduced CD8 positivity, and inhibited $CD8^+$ T activation (Figures 8F-8J). These results further suggested that silencing miR-148a-3p inhibited the malignant progression of CRC by modulating KLF4 and suppressed the immune escape of tumor cells.

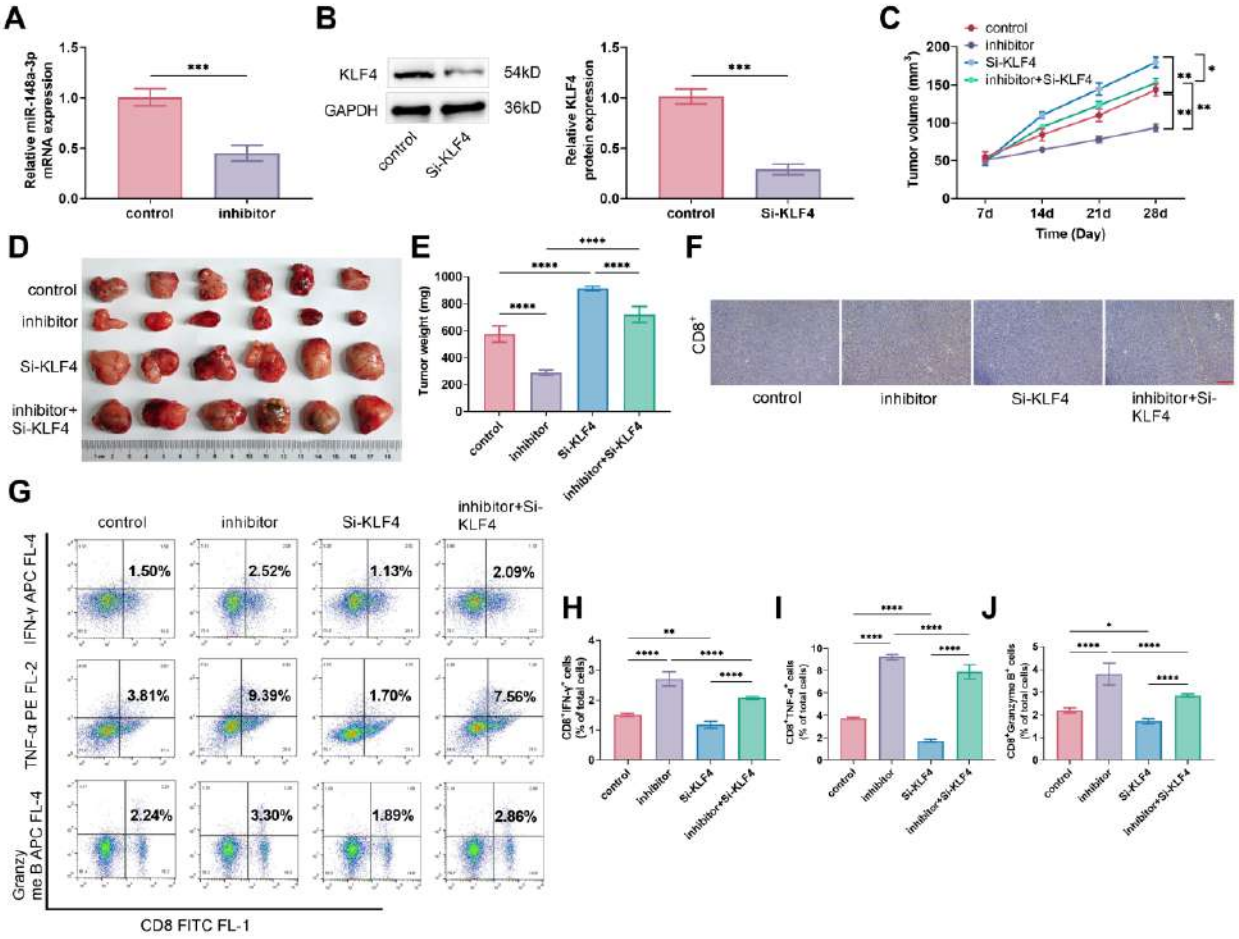

Figure 8. Silencing microRNA (miR)-148a-3p inhibits tumorigenicity and immune escape of colorectal cancer (CRC) cells in vivo. A. After being transfected with inhibitor-NC (control) or inhibitor, the expression of miR-148a-3p was assessed by qRT-PCR. B. After being transfected with Si-NC (control) or Si-kruppel-like transcription factor 4 (KLF4), the expression of KLF4 was assessed by western blot. C. After receiving a subcutaneous injection of 200 µL of LoVo cell suspension transfected with inhibitor-NC + Si-NC (control), inhibitor, Si-KLF4, or inhibitor+Si-KLF4 in the right axilla, respectively. The size of the subcutaneous tumor was measured with vernier calipers at days 7, 14, 21, and 28. D–E. On day 28, the mice were killed, the tumors were weighed and photographed. F. $CD8^+$ T cell infiltration in tumor tissues was detected by immunohistochemistry (20×, bar=100 µm). G–J. Flow cytometry was used to detect the expression of interferon-γ (IFN-γ), tumor necrosis factor-α (TNF-α), and granzyme B in $CD8^+$ T cells infiltrated by tumor tissues. *p<0.05, **p<0.01, ***p<0.001, ****p<0.0001

DISCUSSION

CRC has affected about 10% of people worldwide who are diagnosed with cancers, and this proportion is increasing.[4,7] Detecting the CRC-associated molecular biomarkers helps to screen for CRC and to predict and treat this condition. In this work, the miR-148a-3p content in CRC tissue samples and cells was observed to be significantly upregulated, suggesting a possibility for miR-148a-3p to regulate CRC evolution. Further, miR-148a-3p's biological functions were dug into. As an outcome, excess miR-148a-3p accelerated the immune evasion, EMT, propagation, invasion, and migration of CRC cells. These outcomes contribute to guiding the clinical treatment and diagnosis of CRC.

MicroRNAs can attach to the corresponding target mRNA directly to affect many diseases.[35] Based on bioinformatics tools and experimental validation, KLF4 was ascertained as miR-148a-3p's target gene. As reported, KLF4 functions as an evolutionarily conserved

zinc-finger transcription factor capable of regulating cellular processes (e.g., cell growth, propagation, and differentiation);[36] microRNA is an important factor regulating KLF4 expression in cells. KLF4 can maintain intestinal epithelium in a normal homeostasis state[37] and is under-expressed in cancer cells.[38-47] Once expressed excessively, KLF4 can reduce the tumorigenicity of *in vivo* gastric cancer and colon cancer cells;[48,49] also, KLF4 can inhibit in vitro lung cancer cells to propagate and cloning.[50,51] Additionally, KLF4 can drive cellular EMT by promoting cancer cells' migration and required cytokines' expression,[52,53] or re-stimulate the functions of exhausted effector T cells, thereby boosting anti-tumor immune responses, further improving cancer patients' survival rates.[26] Through this research, the KLF4 level was found in inverse proportion to the miR-148a-3p level; KLF4 was dampened in CRC cells; when expressed excessively, KLF4 restrained the immune evasion and EMT of CRC cells.

EMT is a cellular process affecting the progression of malignant tumors. Through this process, interactions both among cells and between cells and the extracellular matrix are redefined, facilitating the detachment of epithelial cells from their neighbors and the basement membrane. This initiates new transcriptional programs, encouraging the production of mesenchymal tissue.[54] EMT constitutes a significant biological process through which cancerous epithelial cells are transformed, gaining the capabilities to migrate and attack. Its main characteristics include the reduction of epithelial cell markers (represented by E-cadherin and cytokeratins) and the increase of mesenchymal cell markers (represented by vimentin, fibronectin, and N-cadherin).[39,55] The present study findings reveal that excess miR-148a-3p prevented the KLF4 expression in CRC cells and caused down-regulated E-cadherin contents and up-regulated vimentin and N-cadherin contents. This proves that excess miR-148a-3p enhances CRC cells' EMT progression, which might be the reason why CRC cells were enhanced to propagate, attack, and migrate.

Capable of identifying and eliminating cancer cells, T cells play an immune function across various tissues and organs. $CD8^+$ T cells are effective cytotoxic effector cells in anti-tumor immunity, also known as Tc cells.[56] By attaching to antigens presented on the surface of nucleated cells by MHC class I molecules, Tc cells can recognize their targets. During antigen-specificity activation, the affinity between CD8 molecules and MHC molecules helps maintain a close binding between Tc cells and their target cells. In addition to $CD8^+$ T, $CD4^+$ T cells are among the major effector T cells.[57] When $CD8^+$ T and $CD4^+$ T cells recognize their antigens and become activated, several pro-inflammatory cytokines, primarily including TNF-α and IFN-γ, are secreted from these cells to combat tumors, viruses, and microbes;[58-60] additionally, such cells facilitate the death of target cells through the secretion of the serine protease, granzyme B.[61] As detected in the present work, $CD8^+$/$CD4^+$ T cells, after being co-cultured with such CRC cells as having miR-148a-3p overexpressed or KLF4 silenced, exhibited weakened proliferative capacity and increased apoptosis rates, along with a large drop in the levels of granzyme B, IFN-γ, and TNF-α in the supernatant. This variation proves that excess miR-148a-3p might, by retarding the KLF4 expression, impair effector T cells' antitumor effect, further facilitating CRC cells' immune evasion.

This article elucidates the regulatory mechanism of intracellular miR-148a-3p on CRC cells' specific biological functions. In details, the miR-148a-3p level was inversely proportional to the KLF4 level; heightening miR-148a-3p led to a decline in the KLF4 level, followed by a great inhibition of the EMT, migration, attacking, immune evasion, and proliferation of CRC cells, which accords with the detected functions of the cells with solely KLF4 silenced; the detected functions of the cells with miR-148a-3p knocked down were also identical to that of the cells with KLF4 over-expressed. Furthermore, in vivo experiments also confirmed that silencing KLF4 reduced the inhibitory effect of silencing miR-148a-3p on tumor growth. Based on these findings, this paper proposes a molecular mechanism to modulate CRC cells' immune evasion and propagation by miR-148a-3p targeting KLF4. This mechanism can be put to use for immunological treatment of CRC.

To conclude, miR-148a-3p promotes CRC cell proliferation, migration, and immune escape *in vivo* and *in vitro* by targeting and negatively regulating KLF4 expression. This study's finding provides a novel approach to CRC treatment. Based on the target miR-148a-3p alone or in combination with other targets, it is viable to better the treatment protocol. Preventing the miR-148a-3p expression in a targeted way may become an effective method of CRC treatment. In the principle of model-informed drug development, it is possible to develop miR-148a-3p-targeted drugs suitable for clinical application and advance the precision treatment

of CRC by means of artificial intelligence and high-throughput sequencing.

STATEMENT OF ETHICS

Not applicable.

FUNDING

Not applicable.

CONFLICT OF INTEREST

The authors declare no conflicts of interest.

ACKNOWLEDGMENTS

Not applicable.

DATA AVAILABILITY

To acquire the data that underpins the results of this study, please contact the corresponding author, Jiafeng Wang.

AI ASSISTANCE DISCLOSURE

No applicable.

REFERENCES

1. Arnold M, Sierra MS, Laversanne M, Soerjomataram I, Jemal A, Bray F. Global patterns and trends in colorectal cancer incidence and mortality. Gut. 2017;66(4):683-91.
2. Phang CW, Karsani SA, Abd Malek SN. Induction of Apoptosis and Cell Cycle Arrest by Flavokawain C on HT-29 Human Colon Adenocarcinoma via Enhancement of Reactive Oxygen Species Generation, Upregulation of p21, p27, and GADD153, and Inactivation of Inhibitor of Apoptosis Proteins. Pharmacogn Mag. 2017;13(Suppl 2):S321-S8.
3. Sung H, Ferlay J, Siegel RL, Laversanne M, Soerjomataram I, Jemal A, et al. Global Cancer Statistics 2020: GLOBOCAN Estimates of Incidence and Mortality Worldwide for 36 Cancers in 185 Countries. CA Cancer J Clin. 2021;71(3):209-49.
4. Xia C, Dong X, Li H, Cao M, Sun D, He S, et al. Cancer statistics in China and United States, 2022: profiles, trends, and determinants. Chin Med J (Engl). 2022;135(5):584-90.
5. Loree JM, Kopetz S. Recent developments in the treatment of metastatic colorectal cancer. Ther Adv Med Oncol. 2017;9(8):551-64.
6. Li Y, He M, Zhou Y, Yang C, Wei S, Bian X, et al. The Prognostic and Clinicopathological Roles of PD-L1 Expression in Colorectal Cancer: A Systematic Review and Meta-Analysis. Front Pharmacol. 2019;10:139.
7. Siegel RL, Miller KD, Wagle NS, Jemal A. Cancer statistics, 2023. CA Cancer J Clin. 2023;73(1):17-48.
8. Sadri F, Rezaei Z. Noncoding RNAs: Key Modulators of the Hippo Pathway in Hepatocellular Carcinoma Progression. J Can Biomol Therap. 2025;2(1):73-88.
9. Zhao R, Zhao D, Zhu X, Li F, Xiong P, Li S, et al. The Influence of miR-3149 on the Malignancy Progression of Gastric Cancer by Negatively Regulating CEACAM5. J Can Biomol Therap. 2024;1(1):1-10.
10. Liu L, Wang Q, Qiu Z, Kang Y, Liu J, Ning S, et al. Noncoding RNAs: the shot callers in tumor immune escape. Signal Transduct Target Ther. 2020;5(1):102.
11. Omar HA, El-Serafi AT, Hersi F, Arafa EA, Zaher DM, Madkour M, et al. Immunomodulatory MicroRNAs in cancer: targeting immune checkpoints and the tumor microenvironment. FEBS J. 2019;286(18):3540-57.
12. Yi M, Xu L, Jiao Y, Luo S, Li A, Wu K. The role of cancer-derived microRNAs in cancer immune escape. J Hematol Oncol. 2020;13(1):25.
13. Calin GA, Sevignani C, Dumitru CD, Hyslop T, Noch E, Yendamuri S, et al. Human microRNA genes are frequently located at fragile sites and genomic regions involved in cancers. Proc Natl Acad Sci U S A. 2004;101(9):2999-3004.
14. Lin S, Gregory RI. MicroRNA biogenesis pathways in cancer. Nat Rev Cancer. 2015;15(6):321-33.
15. Ye Z, Jiang Y, Wu J. A novel necroptosis-associated miRNA signature predicting prognosis of endometrial cancer and correlated with immune infiltration. Taiwan J Obstet Gynecol. 2023;62(2):291-8.
16. Cao Y, Jiao N, Sun T, Ma Y, Zhang X, Chen H, et al. CXCL11 Correlates With Antitumor Immunity and an Improved Prognosis in Colon Cancer. Front Cell Dev Biol. 2021;9:646252.
17. Chen X, Wang YW, Gao P. SPIN1, negatively regulated by miR-148/152, enhances Adriamycin resistance via upregulating drug metabolizing enzymes and transporter in breast cancer. J Exp Clin Cancer Res. 2018;37(1):100.
18. Dawood AA, Saleh AA, Elbahr O, Gohar SF, Habieb MS. Inverse relationship between the level of miRNA

148a-3p and both TGF-beta1 and FIB-4 in hepatocellular carcinoma. Biochem Biophys Rep. 2021;27:101082.
19. Idichi T, Seki N, Kurahara H, Fukuhisa H, Toda H, Shimonosono M, et al. Molecular pathogenesis of pancreatic ductal adenocarcinoma: Impact of passenger strand of pre-miR-148a on gene regulation. Cancer Sci. 2018;109(6):2013-26.
20. Jung KH, Zhang J, Zhou C, Shen H, Gagea M, Rodriguez-Aguayo C, et al. Differentiation therapy for hepatocellular carcinoma: Multifaceted effects of miR-148a on tumor growth and phenotype and liver fibrosis. Hepatology. 2016;63(3):864-79.
21. Komatsu S, Imamura T, Kiuchi J, Takashima Y, Kamiya H, Ohashi T, et al. Depletion of tumor suppressor miRNA-148a in plasma relates to tumor progression and poor outcomes in gastric cancer. Am J Cancer Res. 2021;11(12):6133-46.
22. Wang W, Dong J, Wang M, Yao S, Tian X, Cui X, et al. miR-148a-3p suppresses epithelial ovarian cancer progression primarily by targeting c-Met. Oncol Lett. 2018;15(5):6131-6.
23. Mreich E, Chen XM, Zaky A, Pollock CA, Saad S. The role of Kruppel-like factor 4 in transforming growth factor-beta-induced inflammatory and fibrotic responses in human proximal tubule cells. Clin Exp Pharmacol Physiol. 2015;42(6):680-6.
24. Sevilla LM, Latorre V, Carceller E, Boix J, Vodak D, Mills IG, et al. Glucocorticoid receptor and Klf4 co-regulate anti-inflammatory genes in keratinocytes. Mol Cell Endocrinol. 2015;412:281-9.
25. Zahlten J, Herta T, Kabus C, Steinfeldt M, Kershaw O, Garcia P, et al. Role of Pneumococcal Autolysin for KLF4 Expression and Chemokine Secretion in Lung Epithelium. Am J Respir Cell Mol Biol. 2015;53(4):544-54.
26. Nah J, Seong RH. Kruppel-like factor 4 regulates the cytolytic effector function of exhausted CD8 T cells. Sci Adv. 2022;8(47):eadc9346.
27. Dong M, Xie Y, Xu Y. miR-7-5p regulates the proliferation and migration of colorectal cancer cells by negatively regulating the expression of Kruppel-like factor 4. Oncol Lett. 2019;17(3):3241-6.
28. Lv H, Zhang Z, Wang Y, Li C, Gong W, Wang X. MicroRNA-92a Promotes Colorectal Cancer Cell Growth and Migration by Inhibiting KLF4. Oncol Res. 2016;23(6):283-90.
29. Mao Q, Quan T, Luo B, Guo X, Liu L, Zheng Q. MiR-375 targets KLF4 and impacts the proliferation of colorectal carcinoma. Tumour Biol. 2016;37(1):463-71.
30. Shang Y, Zhu Z, Zhang Y, Ji F, Zhu L, Liu M, et al. MiR-7-5p/KLF4 signaling inhibits stemness and radioresistance in colorectal cancer. Cell Death Discov. 2023;9(1):42.
31. Zhai F, Cao C, Zhang L, Zhang J. miR-543 promotes colorectal cancer proliferation and metastasis by targeting KLF4. Oncotarget. 2017;8(35):59246-56.
32. Zhao W, Hisamuddin IM, Nandan MO, Babbin BA, Lamb NE, Yang VW. Identification of Kruppel-like factor 4 as a potential tumor suppressor gene in colorectal cancer. Oncogene. 2004;23(2):395-402.
33. Zhang C, Zhang C, Liu X, Sun W, Liu H. Circular RNA PGPEP1 induces colorectal cancer malignancy and immune escape. Cell cycle (Georgetown, Tex). 2023;22(14-16):1743-58.
34. Zheng J, Yang T, Gao S, Cheng M, Shao Y, Xi Y, et al. miR-148a-3p silences the CANX/MHC-I pathway and impairs CD8(+) T cell-mediated immune attack in colorectal cancer. FASEB J. 2021;35(8):e21776.
35. Felekkis K, Touvana E, Stefanou C, Deltas C. microRNAs: a newly described class of encoded molecules that play a role in health and disease. Hippokratia. 2010;14(4):236-40.
36. Ghaleb AM, Yang VW. Kruppel-like factor 4 (KLF4): What we currently know. Gene. 2017;611:27-37.
37. Ghaleb AM, McConnell BB, Kaestner KH, Yang VW. Altered intestinal epithelial homeostasis in mice with intestine-specific deletion of the Kruppel-like factor 4 gene. Dev Biol. 2011;349(2):310-20.
38. Feng F, Liu H, Chen A, Xia Q, Zhao Y, Jin X, et al. miR-148-3p and miR-152-3p synergistically regulate prostate cancer progression via repressing KLF4. J Cell Biochem. 2019;120(10):17228-39.
39. He Z, He J, Xie K. KLF4 transcription factor in tumorigenesis. Cell Death Discov. 2023;9(1):118.
40. Hu D, Gur M, Zhou Z, Gamper A, Hung MC, Fujita N, et al. Interplay between arginine methylation and ubiquitylation regulates KLF4-mediated genome stability and carcinogenesis. Nat Commun. 2015;6:8419.
41. Jiang Z, Zhang Y, Chen X, Wu P, Chen D. Long non-coding RNA LINC00673 silencing inhibits proliferation and drug resistance of prostate cancer cells via decreasing KLF4 promoter methylation. J Cell Mol Med. 2020;24(2):1878-92.
42. Leng Z, Li Y, Zhou G, Lv X, Ai W, Li J, et al. Kruppel-like factor 4 regulates stemness and mesenchymal properties of colorectal cancer stem cells through the TGF-beta1/Smad/snail pathway. J Cell Mol Med. 2020;24(2):1866-77.

43. Qiu Z, Tu L, Hu X, Zhou Z, Lin Y, Ye L, et al. A Preliminary Study of miR-144 Inhibiting the Stemness of Colon Cancer Stem Cells by Targeting Kruppel-Like Factor 4. J Biomed Nanotechnol. 2020;16(7):1102-9.
44. Tian Y, Luo A, Cai Y, Su Q, Ding F, Chen H, et al. MicroRNA-10b promotes migration and invasion through KLF4 in human esophageal cancer cell lines. J Biol Chem. 2010;285(11):7986-94.
45. Wei D, Wang L, Yan Y, Jia Z, Gagea M, Li Z, et al. KLF4 Is Essential for Induction of Cellular Identity Change and Acinar-to-Ductal Reprogramming during Early Pancreatic Carcinogenesis. Cancer Cell. 2016;29(3):324-38.
46. Xue M, Zhou C, Zheng Y, Zhang Z, Wang S, Fu Y, et al. The association between KLF4 as a tumor suppressor and the prognosis of hepatocellular carcinoma after curative resection. Aging (Albany NY). 2020;12(15):15566-80.
47. Zhang C, Liu J, Zhang Y, Luo C, Zhu T, Zhang R, et al. LINC01210 accelerates proliferation, invasion and migration in ovarian cancer through epigenetically downregulating KLF4. Biomed Pharmacother. 2019;119:109431.
48. Zhang N, Zhang J, Shuai L, Zha L, He M, Huang Z, et al. Kruppel-like factor 4 negatively regulates beta-catenin expression and inhibits the proliferation, invasion and metastasis of gastric cancer. Int J Oncol. 2012;40(6):2038-48.
49. Patel NV, Ghaleb AM, Nandan MO, Yang VW. Expression of the tumor suppressor Kruppel-like factor 4 as a prognostic predictor for colon cancer. Cancer Epidemiol Biomarkers Prev. 2010;19(10):2631-8.
50. Hu W, Hofstetter WL, Li H, Zhou Y, He Y, Pataer A, et al. Putative tumor-suppressive function of Kruppel-like factor 4 in primary lung carcinoma. Clin Cancer Res. 2009;15(18):5688-95.
51. Zhou Y, Hofstetter WL, He Y, Hu W, Pataer A, Wang L, et al. KLF4 inhibition of lung cancer cell invasion by suppression of SPARC expression. Cancer Biol Ther. 2010;9(7):507-13.
52. Dong P, Kaneuchi M, Watari H, Hamada J, Sudo S, Ju J, et al. MicroRNA-194 inhibits epithelial to mesenchymal transition of endometrial cancer cells by targeting oncogene BMI-1. Mol Cancer. 2011;10:99.
53. Kumar M, Allison DF, Baranova NN, Wamsley JJ, Katz AJ, Bekiranov S, et al. NF-kappaB regulates mesenchymal transition for the induction of non-small cell lung cancer initiating cells. PLoS One. 2013;8(7):e68597.
54. Dongre A, Weinberg RA. New insights into the mechanisms of epithelial-mesenchymal transition and implications for cancer. Nat Rev Mol Cell Biol. 2019;20(2):69-84.
55. Mittal V. Epithelial Mesenchymal Transition in Tumor Metastasis. Annu Rev Pathol. 2018;13:395-412.
56. Reiser J, Banerjee A. Effector, Memory, and Dysfunctional CD8(+) T Cell Fates in the Antitumor Immune Response. J Immunol Res. 2016;2016:8941260.
57. Zeng Z, Chew HY, Cruz JG, Leggatt GR, Wells JW. Investigating T Cell Immunity in Cancer: Achievements and Prospects. Int J Mol Sci. 2021;22(6).
58. Chen Y, Xu J, Wu X, Yao H, Yan Z, Guo T, et al. CD147 regulates antitumor CD8(+) T-cell responses to facilitate tumor-immune escape. Cell Mol Immunol. 2021;18(8):1995-2009.
59. Jansen CS, Prokhnevska N, Master VA, Sanda MG, Carlisle JW, Bilen MA, et al. An intra-tumoral niche maintains and differentiates stem-like CD8 T cells. Nature. 2019;576(7787):465-70.
60. Jhunjhunwala S, Hammer C, Delamarre L. Antigen presentation in cancer: insights into tumour immunogenicity and immune evasion. Nat Rev Cancer. 2021;21(5):298-312.
61. Shi Z, Du Q, Wang X, Wang J, Chen H, Lang Y, et al. Granzyme B in circulating CD8+ T cells as a biomarker of immunotherapy effectiveness and disability in neuromyelitis optica spectrum disorders. Front Immunol. 2022;13:1027158.